ELSEVIER

Biophysical Chemistry 98 (2002) 35–48

Biophysical Chemistry

www.elsevier.com/locate/bpc

Hydration, slaving and protein function

Hans Frauenfelder[a], P.W. Fenimore[a,*], B.H. McMahon[b]

[a]*Center for Non-linear Studies, MS B258, Los Alamos National Laboratory, Los Alamos, NM 87545, USA*
[b]*T-10, MS K710, Los Alamos National Laboratory, Los Alamos, NM 87545, USA*

Received 19 September 2001; received in revised form 1 November 2001; accepted 1 November 2001

Abstract

Protein dynamics is crucial for protein function. Proteins in living systems are not isolated, but operate in networks and in a carefully regulated environment. Understanding the external control of protein dynamics is consequently important. Hydration and solvent viscosity are among the salient properties of the environment. Dehydrated proteins and proteins in a rigid environment do not function properly. It is consequently important to understand the effect of hydration and solvent viscosity in detail. We discuss experiments that separate the two effects. These experiments have predominantly been performed with wild-type horse and sperm whale myoglobin, using the binding of carbon monoxide over a broad range of temperatures as a tool. The experiments demonstrate that data taken only in the physiological temperature range are not sufficient to understand the effect of hydration and solvent on protein relaxation and function. While the actual data come from myoglobin, it is expected that the results apply to most or all globular proteins.

Keywords: Myoglobin; Protein dynamics; Protein function; Solvent influence; Hydration; Trehalose

1. Introduction

Protein in living systems work in networks that may contain as many as a few thousand proteins [1–4]. Such a network can be effective only if the function of an individual protein is not immutable, but can be influenced by external factors, such as protein–protein and nucleic acid–protein interactions, or by the effect of small molecules, such as lactate. The study of the dynamics and function of proteins under the influence of external agents is consequently an important task. In the present review, we discuss two relevant agents, hydration and viscosity. Both are controlled by the medium surrounding the proteins. One reason for this discussion is the fact that special and unique qualities have been attributed to one particular medium, trehalose [5–7]. We show, using data available in the literature, that hydration and solvent viscosity both have to be varied in order to understand the phenomena observed.

Myoglobin (Mb) is the protein that we use to discuss the effects of hydration and viscosity. Mb has long served as a model. It was the first protein for which the structure was determined [8]. Maurizio Brunori has contributed essential insights into the study of the function of Mb [9,10]. Long

*Corresponding author. Tel.: +1-505-667-9956.
E-mail address: fenimore@cnls.lanl.gov (P.W. Fenimore).

0301-4622/02/$ - see front matter
PII: S0301-4622(02)00083-2

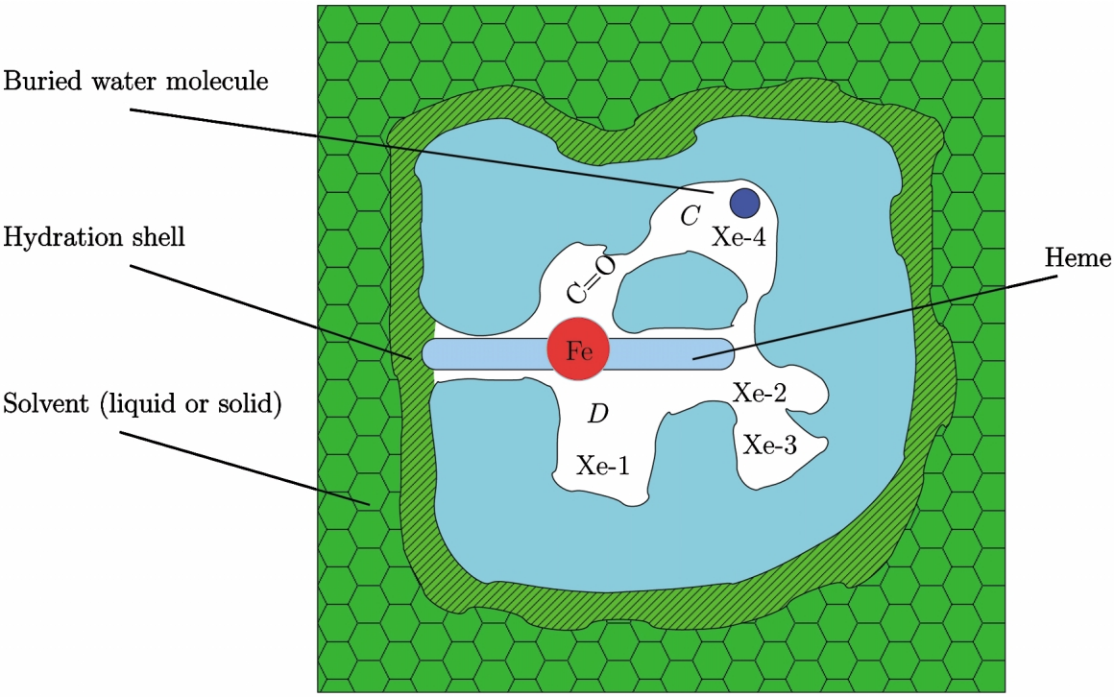

Fig. 1. Myoglobin, the model: the cross-section shows the protein, the heme group with the central iron atom, a number of cavities, the hydration shell, some internal water and the solvent (liquid or solid).

considered just a storage protein, Mb is actually an allosteric enzyme. At high pH, it acts as a dioxygen storage protein; at low pH, it behaves like an enzyme involved with NO [11,12]. Here we use the binding of carbon monoxide (CO) to Mb [13] to discuss the effect of hydration and viscosity on biological function. A cross-section through Mb is sketched in Fig. 1. At the heart of Mb is a heme group, with a central iron atom and four *custom-made* cavities, Xe-1 to Xe-4 [14,15]. The protein is surrounded by the hydration shell, a thin layer of water [16–23]. In addition, a number of water molecules are buried inside [24–27]. The external and internal water molecules and the solvent viscosity are important for protein motion [28–34].

The binding of CO to Mb is studied by flash photolysis. The system is initially in the bound state, MbCO, as indicated in Fig. 1. A laser flash breaks the bond between the iron and the CO, and the CO moves away from the heme. The motion of the CO is followed by spectroscopically measuring $N(t)$, the fraction of Mb molecules that have not rebound a CO at the time t after the flash. Typical kinetic curves are shown in Fig. 2 [35]. At low temperatures, the CO moves only a few Å and rebinds in a single step. At high temperatures, the CO escapes into the solvent and rebinds from there. The steps involved in rebinding can be described by the equation [13]:

$$A \leftarrow B \rightleftharpoons C \rightleftharpoons D \rightleftharpoons S \quad (1)$$

that is represented schematically in the reaction landscape in Fig. 3a. A denotes the bound state, S the state with CO in the solvent, and B, C and D are intermediate states. Kinetics, of course, gives no structural information. Such information comes from X-ray diffraction data [36–41]. These show that in B, the CO is in the heme pocket, and in D it has moved to the proximal side into the Xe-1 cavity. In C, the CO may be in Xe-4. Sperm whale

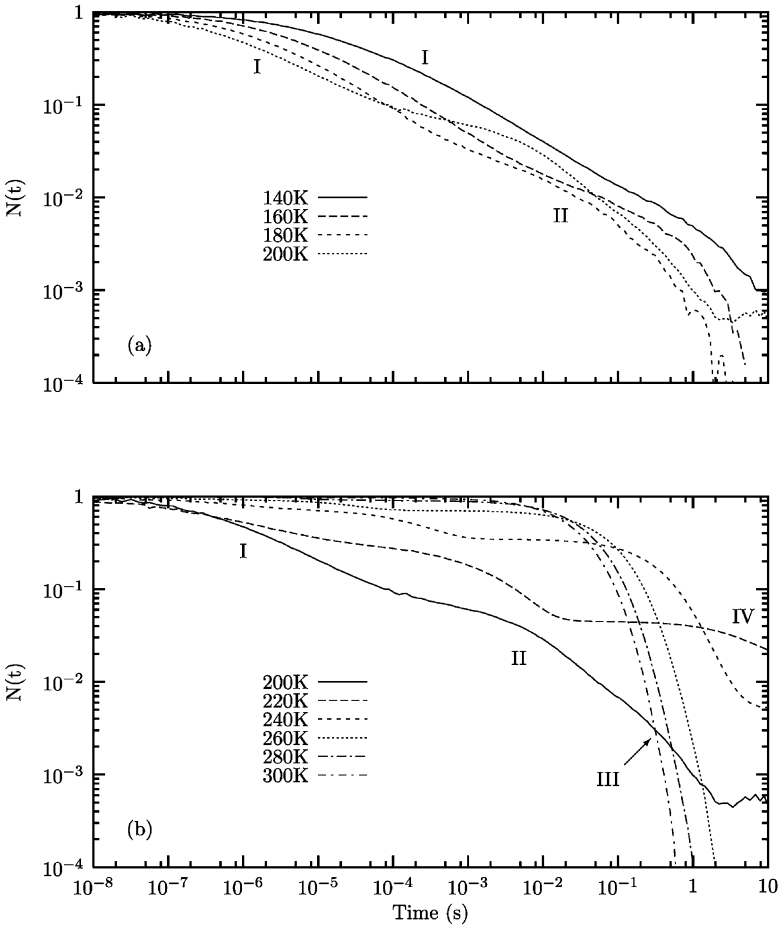

Fig. 2. Kinetics of CO recombination to horse myoglobin from 140 to 300 K [35]. The sample is 500 mM KCl, pH 9.0 and 3:1 glycerol/water.

(swMb) and horse heart Mb (hMb) behave somewhat differently. In hMb, position C is difficult to observe kinetically. In the following we discuss how hydration and solvent viscosity affect the various steps in the scheme in Eq. (1). Three remarks should be added to Eq. (1) and Fig. 2. In a number of papers (e.g. [42]), Eq. (1) has been extended by adding branching. Branching can certainly not be excluded, but we can fit the data over the entire temperature range (40–300 K) without using such branching. We therefore do not include it in the discussion. The second remark again concerns the relevance of studies covering the entire temperature range, from below 200 to 300 K. As Fig. 2 shows, the fraction of CO that escapes into the solvent is very close to 1 near ambient temperature. The unimolecular (i.e. geminate) transitions in Eq. (1) are therefore nearly indistinguishable; separating them at high temperatures requires taking the difference of two large numbers. Systematic extrapolation starting from low temperatures is needed to unambiguously separate the various steps. The third remark concerns the role that studies on mutant Mb played in establishing the location of the intermediates C and D in Eq. (1). Such studies were indeed relevant, but the unambiguous assignment has come from X-ray data.

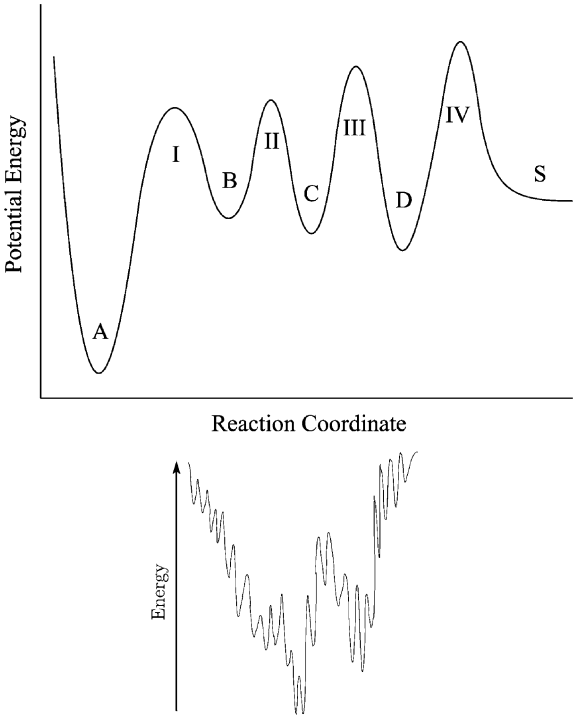

Fig. 3. (a) The reaction landscape for the binding of CO to swMb, as deduced from flash photolysis experiments [13]. (b) A schematic cross-section through the energy (conformation) landscape. The landscape is a construct in $3N-3$ co-ordinates, where N is the number of atoms in the protein and the hydration shell. A point in this landscape describes the positions of all atoms in a given substate.

We wish to understand and distinguish protein dynamics and ligand migration. This is accomplished in a controlled fashion by varying temperature, solvent viscosity, etc. The interpretation of the function of proteins is clarified through the concept of an energy or conformation landscape [13,43,44]: a given protein can assume a very large number of different, but usually related, structures. The multitude of these conformational substates is described by the energy landscape, a construct in a space of $3N-3$ dimensions, where N is the number of atoms in the protein and its hydration shell. A simplified one-dimensional cross-section through such an energy landscape is sketched in Fig. 3b. Each location on the energy landscape characterizes the positions of all atoms of the protein and of the hydration shell. The energy landscape is hierarchically organized into a number of tiers, which are characterized for instance by the average barrier height between substates [45]. Of interest here are the top two tiers, 0 and 1. Tier 0 describes a small number of measurably different conformations, called taxonomic substates, which can have different functions [11]. In Fig. 3b, two such taxonomic substates are shown. Mb has three taxonomic substates, called A_0, A_1 and A_3 [46,47]. A_1 dominates at high pH and is involved in dioxygen storage. A_0 dominates at low pH and may perform NO enzymatics [10,11]. Initially, the taxonomic substates were defined through the infrared stretch frequencies. X-ray data now show that in A_0 the protonated distal histidine has moved out from the heme pocket [48]. The structure of A_3 is still not known. Each taxonomic substate can assume a very large number of tier-1 statistical substates. These substates all perform the same function, but at different rates. At temperatures below the so-called protein glass temperature, T_g, the frozen heterogeneity of the statistical substates gives rise to non-exponential time-dependent relaxation and reaction phenomena [49]. Each statistical substate may again contain substates of lower tiers, the function of which is not yet clear.

The existence of statistical substates is observed in the non-exponential low-temperature binding of CO, as depicted in Fig. 2 below approximately 180 K. A multi-flash experiment proved, in a primitive version of a single-molecule technique, that the non-exponential time dependence is caused by inhomogeneity [13]: at these low temperatures each protein rebinds exponentially, but proteins in different substates do so with different binding rates. The different binding rates can be attributed to different barrier heights, H, for binding to the heme iron. The non-exponential time dependence of rebinding can consequently be written as an integral over contributions from proteins with different barrier heights H:

$$N(t)=\int g(H)\exp\{-k(H)t\}\ \mathrm{d}H \qquad (2)$$

where H is the height of the enthalpy barrier for the step $B\rightarrow A$, $g(H)\mathrm{d}H$ the probability of finding

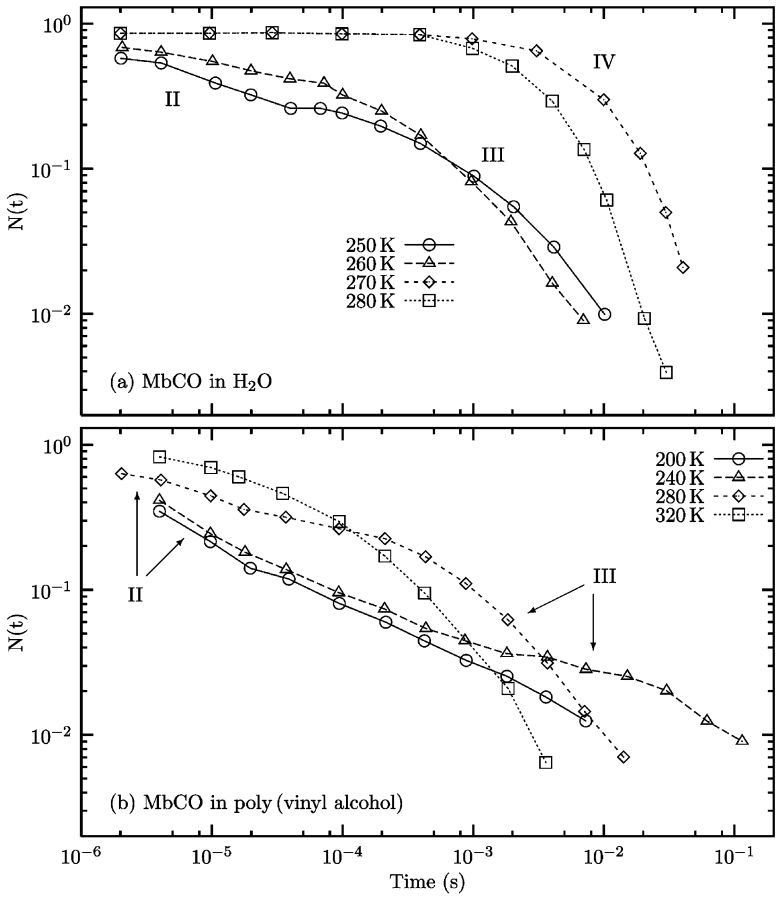

Fig. 4. (a) Rebinding of CO to Mb in water (ice) from [13]. Above the melting point (270 K), binding is exponential in time and proportional to the CO concentration in the water. Below the freezing point, CO can no longer escape from the protein interior and binding is non-exponential in time. 'II' and 'III' denote kinetics processes two (mostly C→A) and three (mostly D→A). (b) Binding of CO to Mb embedded in solid PVA [13]. CO cannot escape into the solvent and binding is non-exponential in time.

a barrier with height between H and $H+\mathrm{d}H$, and $k(H)=A(T/T_0)\exp(-H/RT)$ the relevant Arrhenius rate coefficient. T_0 is an arbitrary constant, usually taken to be 100 K. Eq. (2) fits the CO binding data for the three taxonomic substates A_0, A_1 and A_3 over the range from approximately 40 to 180 K with different enthalpy distributions and different pre-exponential factors [50].

2. Data

In this section, we present data culled from our own and from related work. Fig. 2 shows $N(t)$ for the binding of CO to hMb at temperatures below (Fig. 2a) and above (Fig. 2b) 200 K [35]. $N(t)$ denotes the fraction of the Mb molecules that have not rebound a CO molecule at time t after photodissociation. Fig. 4 gives the recombination kinetics of CO to sperm whale myoglobin for Mb embedded in poly(vinyl alcohol) (PVA), in water, and in ice [13]. Fig. 5 reproduces some of the data taken by Hagen and co-workers of Mb embedded in trehalose [5,6], and by Kleinert and co-workers in a mixture of 92% sucrose–water [34]. Information on the binding process also comes from temperature-derivative spectroscopy (TDS) [51]. In this technique, MbCO is photolyzed at a low temperature, 12 K, where rebinding is extremely

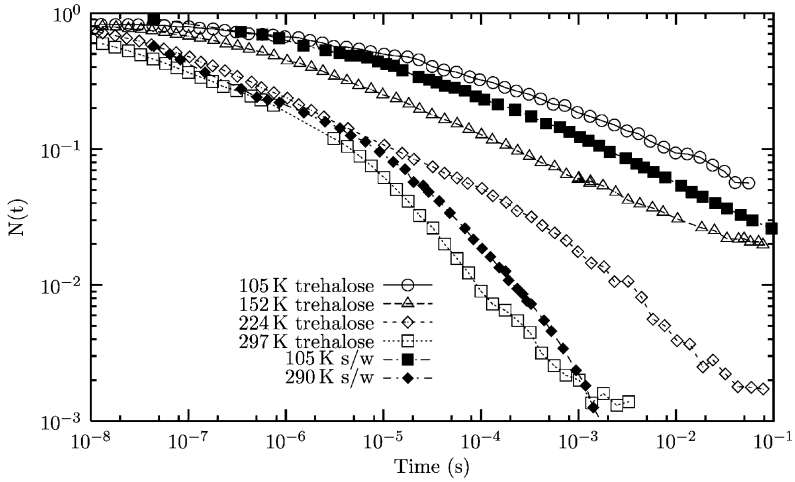

Fig. 5. Binding of CO to Mb embedded in trehalose and in 92% sucrose–water (s/w), The curves for trehalose are taken from Hagen et al. [5,6], and those for sucrose–water from Kleinert et al. [34].

slow. The sample is then slowly heated and rebinding is followed by recording the reformation of MbCO, for instance by observing the infrared spectra of the three taxonomic substates A_0, A_1 and A_3. The result for swMb, shown in Fig. 6a, verifies that rebinding at low temperatures must be described by an activation enthalpy distribution, Eq. (2), and that the distribution is different for the different taxonomic substates. Additional insight comes from Fig. 6b. In this experiment, the sample was first cooled from 160 to 12 K under illumination. The TDS experiment was then started at 12 K and rebinding was observed up to approximately 140 K [52]. Rebinding from the three states B, C and D, introduced in Eq. (1), can be clearly observed. In hMbCO, state C is barely observable. Protein motion and the migration of a ligand through the protein depend, for instance, on the viscosity of the medium in which the protein is embedded. Fig. 7, taken from Beece et al. [30] and Ansari et al. [31,34], shows the dependence on solvent viscosity of three characteristic processes, exit and entry of the CO from the protein ($D \rightleftharpoons S$), and migration of the CO from D to C. Also shown in this figure is the rate coefficient for the process $D \rightarrow C$ in PVA. PVA prevents the entry and exit of CO, and therefore no corresponding point is shown. Fig. 8 compares the process $S \rightarrow A$ in water at 270 K with process III ($D \rightarrow A$) at 250 K in ice and in 75% glycerol–water (g/w). To obtain the curve for g/w, the rebinding from the solvent has been subtracted from the data points measured (Fig. 2) and the rate coefficient has been corrected for the escape process $D \rightarrow S$.

3. Data interpretation—hydration

In 1975, the multi-well model summarized by Eq. (1) described the kinetic data obtained over extended ranges of time and temperature tolerably well [13]. The structural interpretation, however, was guesswork. Studies with mutants suggested that the CO could be in Xe-4, but solid information came from sophisticated X-ray diffraction experiments. Using the results of TDS experiments, such as those shown in Fig. 6b [52], the X-ray data provide the structural information sketched in Fig. 1: in state B, the CO is still in the heme pocket, parallel to the heme plane and approximately 4 Å from the center of the heme group. In C, the CO is most likely in the Xe-4 cavity. In D the CO has moved to the proximal side into the largest cavity, Xe-1. These assignments have been tested by measuring the binding of CO in the presence of Xe ([53] and Chu et al., in preparation): Xe slows the transit of CO to Xe-1.

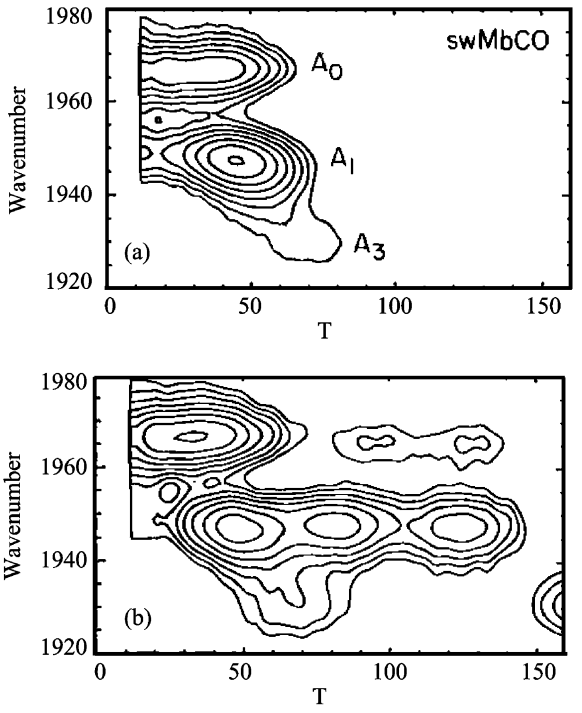

Fig. 6. Binding of CO to swMb at pH 6.0, using temperature-derivative spectroscopy (TDS) [51,52]. (a) Binding after a single photoflash at 12 K. The temperature was then increased at a constant rate (3.125 mK s^{-1}) and the binding was monitored at the stretch frequencies of the bound CO and depicted as contour maps. (b) TDS contours after cooling under constant illumination from 160 to 12 K [52].

Most of the photodissociation experiments have been performed with the MbCO embedded in a 75% glycerol–water solvent [13,35]. In this solvent the transition from B to A dominates up to approximately 200 K, as is evident in Fig. 2a. Above approximately 150 K, CO begins to move to C and D. Above approximately 200 K CO can also escape into the solvent. In Fig. 2, these processes are denoted by I–IV: Process I is the direct binding, B→A. Process II involves C→B and C→D. Process III describes both escape into the solvent and rebinding, and process IV is binding from the solvent.

Quantitative evaluation of the data shows that binding from D to A slows by a factor of approximately 30 above 230 K [35]. We ascribe this slowing to a shift of the distal histidine [24–28] and possibly to a water molecule entering after CO has left [54].

With this background, we turn to the effect of hydration on ligand binding. Fig. 5 shows the binding of CO to Mb embedded in trehalose [5,6] and 92% sucrose–water [34] at several temperatures. Rebinding is non-exponential up to nearly 300 K and only the direct binding to A, B→A, is apparent. Transitions to C and D are essentially absent up to the highest temperatures measured. $N(t)$ can be fitted with Eq. (2) up to approximately 300 K and the resulting distribution function $g(H)$ is similar to the $g(H)$ that reproduces process I for the binding to Mb in glycerol–water [13]. What is going on here? To understand, we present in Fig. 4 data for the CO binding in water, in ice, and in solid poly(vinyl alcohol) [13]. In water (Fig. 4a) rebinding from the solvent (process IV) dominates. As soon as the sample freezes, the solvent process disappears. In contrast to the binding in trehalose and in sucrose–water depicted in Fig. 5, however, processes II and III are visible, and they are non-exponential in time. Thus, the CO can move from the heme pocket to Xe-4 and Xe-1 even in ice, but it can no longer escape into the surroundings. The situation is similar in PVA (Fig. 4b) where processes II (C→A) and III (D→A) appear above 200 K. What causes the difference between trehalose and sucrose–water on one hand, and ice and PVA on the other? The answer is sample preparation. MbCO in trehalose [5,6] and in 92% sucrose–water [34] was dehydrated. The residual water content was 3.5 and 8%, respectively. The data in Fig. 5 thus represent dehydrated MbCO, without all the internal water. In this dehydrated protein, the ligand can still be photodissociated, but it cannot leave state B in the heme pocket. The passage from B to C and D may be blocked because dehydration has changed the structure or has stopped internal motion. In the hydrated protein, in contrast, passage to C and D is possible, even in solid PVA and in ice. Thus, in a hydrated protein near 300 K, transitions in all tiers of the energy landscape take place. In a dehydrated protein, however, transitions among substates of tier 1 are absent or very slow. Otherwise, binding would be an exponential function of time. Transitions between the taxonomic substates

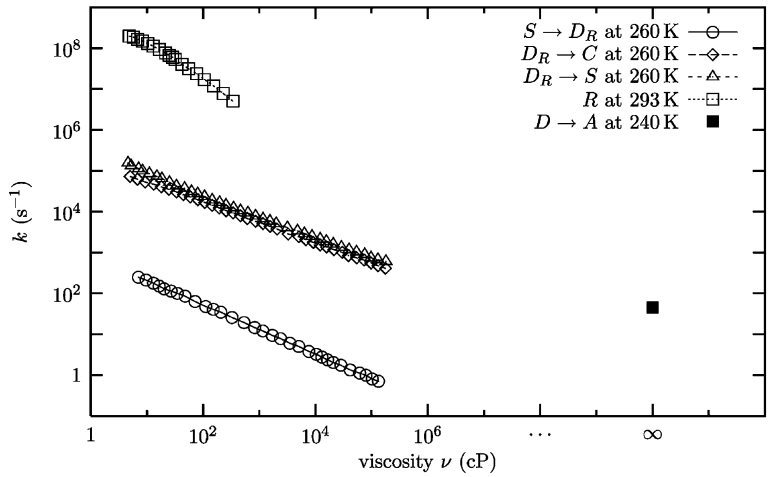

Fig. 7. Viscosity dependence of the rate coefficients in MbCO of the exit ($D_R \rightarrow S$) and entrance processes ($S \rightarrow D_R$), of the migration from D to C at 260 K [30], and of the protein relaxation R at 293 K [32]. The index R indicates that the protein is relaxed. The filled square labeled $D \rightarrow A$ represents the transition in PVA at 240 K, and corresponds to essentially infinite viscosity. The rate k given for $S \rightarrow D_R$ is the pseudo-first-order rate coefficient and is equal to $r_{\text{biomolecular}} \times 10^{-5}$ mM^{-1}.

A_0 and A_1 are also absent, as has been shown by Cordone and co-workers [7]. Thus, a dehydrated protein is dead. These results imply that it is not trehalose that is responsible for reducing or eliminating conformational motion, but dehydration. Water is necessary for motions in tiers 0 and 1 of the energy landscape.

4. Slaving and viscosity

Proteins in living systems are not isolated; they interact with their environment. In the present section we consider one aspect of this interaction, the effect of the viscosity of the solvent [29–34], or in other words the effect of solvent mobility on

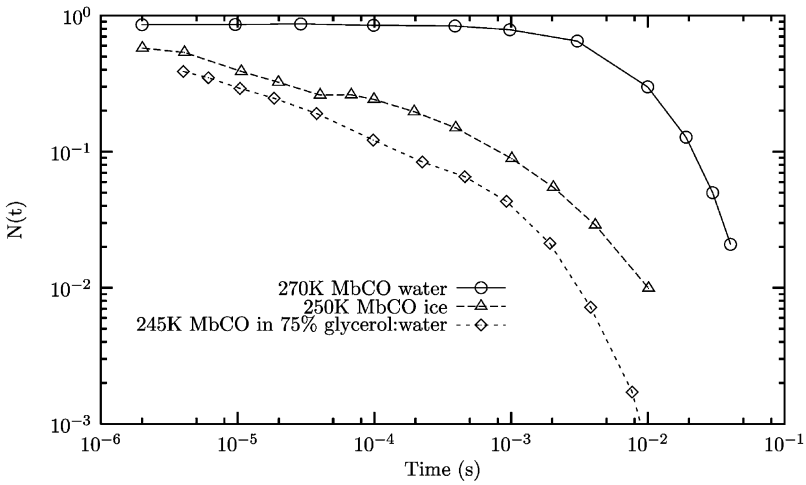

Fig. 8. Selected data [13]. The binding of CO to Mb in water at 270 K corresponds to the process $S \rightarrow A$. The curves for binding in ice and 75% glycerol–water near 250 K describe process III, $D \rightarrow A$. The curve for g/w was obtained by subtracting the solvent process from the total binding curve, and correcting for the fact that a fraction of the CO escapes to the solvent in g/w.

protein mobility [55,56]. Case and Karplus first pointed out that the transitions in Mb described by Eq. (1) could not occur in a rigid protein, but had to involve fluctuations [57]. Such fluctuations can be described as transitions among conformational substates [58,59]. While experimental and theoretical exploration of the organization of the energy landscape and the coupling of transitions in the various tiers is still in its infancy, some general remarks can be made. The energy landscape is hierarchically organized [43,45]. Fluctuations in the different tiers decrease with decreasing temperature. For each tier a glass temperature can be postulated. Below the glass temperature, transitions rates between substates are smaller than, say, 10^{-3} s^{-1}. Transitions among substates in tiers 0 and 1 are strongly coupled to motion in the solvent; they can be called slaved. The glass transitions in these tiers will not only depend on the protein, but also on the solvent and its motion. They can therefore be called *slaved glass transitions* [47]. The Arrhenius relation, normally used by biophysicists and biochemists, does not contain a term that characterizes the motion of the environment; it is consequently not suited to describe phenomena in biomolecules. An equation introduced by Kramers provides insight [60–62]. Kramers showed that escape over a barrier depends on friction. In the low-friction limit, the rate coefficient, k, is proportional to the friction, η. In the high-friction limit, k is proportional to $1/\eta$. Stokes' law implies that the friction coefficient is proportional to the viscosity. We can therefore write for a rate coefficient:

$$k = \text{const}\ \ \eta^{\kappa} \tag{3}$$

where κ can vary from -1 to 1, depending on the magnitude of the viscosity. Viscosity is actually not necessarily the sole or most appropriate property to describe the solvent–protein interaction, as has been pointed out by Yedgar et al. [33]. Nevertheless, we use it here because many measurements have been performed as a function of solvent viscosity. Even for a reaction inside a protein, the effective viscosity is not only a property of the protein, but also depends on the external viscosity. The connection between motion in the solvent and the protein has, in particular, been explored by Doster and collaborators [63,64] and Vitkup et al. [56]. Two different types of motions are distinguished, rapid collisions (10^{13} s^{-1}) that are nearly viscosity-independent, and slower structural fluctuations that depend on viscosity and correspond to transitions among substates. For these slow structural fluctuations, three regimes can be distinguished. At very high external viscosity, some internal protein motion still occurs and is essentially independent of the solvent viscosity. At very low external viscosity, all internal motion is governed by the protein viscosity. In the intermediate region, Eq. (3) with $\kappa \leq 1$ appears to be a good approximation.

The data in Figs. 2, 4, 6–8 display some of these features. In a hydrated protein processes II and III are observable, even in a rigid environment, for example ice or solid PVA, where the viscosity is extremely high. The CO can still move from cavity to cavity. Escape to S, however, is no longer possible. These observations imply that transitions between cavities may be governed by internal fluctuations.

Fluctuations in more than one tier of the substates must be involved in the motion of the CO and the protein relaxation, as can be deduced from the data in Fig. 8. These data demonstrate that transit to Xe-1 (D) and return from there are nearly equally fast in a mobile and a frozen solvent. The rebinding is, however, an exponential function of time in the glycerol–water solvent, but highly non-exponential in ice and solid PVA.

5. Ligand binding, concepts and detours

The binding of CO to Mb, once considered the prototype of a simple one-step reaction, has turned out to be exceedingly complex. After more than 30 years of work by many groups, involving many detours and wrong directions, we believe that the main features are now understood. We can ask three questions: what are these features? What concepts have emerged from the ligand-binding studies? What were the major detours and why were they made? We sketch some answers to these questions.

5.1. Ligand binding

Our present picture of the binding of CO to Mb is close to that introduced in 1975 and described by the scheme in Eq. (1) [13]. Binding involves the states A–S. At temperatures below approximately 200 K, no water molecule enters B (or C) and the motion of CO from D to B is governed by unrelaxed barriers. Above approximately 200 K, however, a water molecule can enter and slow the CO motion. Moreover, the distal histidine, His-64, can change position and further slow the transition to B. We describe this relaxation by a subscript R on D, $D \rightarrow D_R$. Near 300 K, binding still involves the states B, C and D_R, but in most of these solvents transitions among them, and also escape to the solvent, are fast compared to the final binding step $B \rightarrow A$. The rate coefficient k_{BA} for this rate-limiting step still follows the Arrhenius law used for Eq. (2) and is of the order of 10^7 s^{-1}. After photodissociation, the probability, N_S, of escape to the solvent is nearly 1, geminate rebinding is difficult to observe (Fig. 2b), and separating $B \rightarrow A$ from $D \rightarrow A$ is even more difficult. Two remarks follow from this result. First, at these temperatures the various states B, C and D are in quasi-equilibrium. Even if sidepaths exist, they would also be included and the essential results would not be changed. Second, the result again shows that low-temperature data are essential for arriving at a clear picture. Room-temperature data alone do not permit unique assignments.

5.2. Concepts

Proteins are complex systems. The complexity is already apparent from the reaction and the conformational energy landscapes sketched in Fig. 3. Essential concepts that have emerged from studies of ligand binding to myoglobin are: the energy landscape and its organization into a hierarchy [43,44]; the different functions of different taxonomic substates; the multi-step binding as expressed in Figs. 1 and 3a and Eq. (1); the importance of custom-made cavities; the effects of the external solvent (slaving); the hydration shell and internal water molecules; and the necessity of describing protein reactions by a (generalized) Kramers equation. It is likely that these concepts also apply to other proteins and more complex systems. Myoglobin may consequently be a prototype for complex systems in general, and in particular for the exploration of protein functions in networks.

5.3. Detours

The search to understand a physical or biological phenomenon rarely follows a straight path. Detours are unavoidable and can be of two types. Either two different models explain a particular observation equally well, or a real mistake is made, either in the recording or evaluation of data. In either case, additional experiments or simulations can lead to the right path. The story of ligand binding provides a number of examples of detours and we dissect a few here.

5.3.1. Are protein ensembles homogeneous or heterogeneous?

The observation of non-exponential rebinding of CO to Mb at low temperatures, as in Fig. 2, can be explained in two ways. Either each protein rebinds exponentially but different Mb molecules do so with different rates, or all proteins rebind equally but non-exponentially. Multiple flash experiments unambiguously showed that the first model is correct and led to the concept of an energy landscape (Fig. 24 in [13]). Explanations other than the existence of different conformations were put forward, for instance based on anharmonic vibrational spectroscopies [65]. Many additional experiments, however, in particular spectral and kinetic hole-burning, support the concept of an energy or conformation landscape [43,66].

5.3.2. Conformational diffusion or multi-well transitions?

The initial model [13] and the model we now favor involves five wells (A, B, C, D_R and S) on the reaction landscape. Transitions between wells are described by a Kramers-type equation. A different model was introduced in a seminal paper by Agmon and Hopfield [67]. These authors proposed that the kinetically observed states C and D, represented by processes II and III, are in reality

still the same transition B → A, but that the barrier for rebinding increases because of the relaxation of the protein from the bound to the deoxy state. Ligand binding is described as conformational diffusion on an effective, temperature-dependent potential determined by two co-ordinates, the ligand–iron separation and an effective protein co-ordinate. The model has been used by Agmon and collaborators to describe CO binding to Mb embedded in glycerol/water [68] and in trehalose [69]. At one time we also accepted part of this model and showed that it can describe process II well [70]. The two models can be combined. There can be five barriers, as in Eq. (1), but relaxation can increase the barrier between B and A, and thus slow rebinding. Which of these models is correct? The X-ray data imply that states C and D indeed exist and can be identified with Xe-4 and Xe-1. Thus, they rule out a purely relaxational model. States C and D are also kinetically observed in Fig. 6b. Moreover, the quantitative evaluation based on Eq. (1) [35] provides a fit over the entire temperature range that is much better than the fit shown in Figs. 1 and 3 of Sastry and Agmon. Thus, we believe that the model sketched in Section 5.1 is closer to reality and that a model based on diffusion in a temperature-dependent potential cannot explain all the data.

5.3.3. Does the barrier between B and A increase when the protein relaxes?

The question as to whether the barrier between B and A increases because of relaxation from the bound state to the deoxy structure is answered by another argument. The Arrhenius slope of λ_S at high temperatures should show if the barrier H_{BA} has increased upon relaxation. The early data [13] demonstrated that no relaxation takes place; they gave $H_{BA} \approx H(\lambda_S) \approx 10$ kJ mol^{-1}. We assert that the innermost barrier is essentially unaffected by the protein relaxation accompanying the photodissociation. This also implies that the rate coefficient $k_{21} \approx 2 \times 10^5$ s^{-1} measured by Henry et al. at room temperature does not describe B → A, but more likely D → A [71].

5.3.4. Slaving: the effect of the external viscosity

Some detours are still not finished. A quantitative description of the effect of the solvent viscosity is such a case. Eq. (4) indicates that the rate coefficient for a transition will in general depend on viscosity. If such a transition takes place inside the protein, the question arises as to what viscosity will be relevant. Beece et al. [30] neglected the internal viscosity and wrote in effect:

$$k(T,\nu) = \left(\frac{A}{\nu^{\kappa}} + B\right)\exp\left(-\frac{H}{RT}\right) \quad (4)$$

Eaton and collaborators [31,32] assumed the effective viscosity to be the sum of the internal viscosity, σ, and the solvent viscosity, ν, and wrote:

$$k(T,\nu) = \frac{C}{\sigma + \nu}\exp\left(-\frac{H}{RT}\right) \quad (5)$$

Neither relation is satisfactory. Eq. (4) hides the internal viscosity in B and makes an arbitrary assumption about the co-operation between internal and external friction. Eq. (5) predicts vanishing rate coefficients for very large external viscosity. This prediction is contradicted by the observation of internal motion in rigid environments, as for instance shown in Fig. 4. More experimental data and theoretical models are required to solve this problem.

5.3.5. Is trehalose special?

After photodissociation of MbCO embedded in trehalose, Hagen and collaborators [5,6] observed only the final step B → A up to nearly 300 K. They attributed the nearly complete absence of the transition B → C → D to the essentially infinite viscosity of the trehalose glass. Sastry and Agmon evaluated the Hagen experiment and suggested that trehalose prevents 'protein collapse' and preserves the internal protein mobility [69]. The experiments in ice and PVA discussed above imply that these explanations are wrong. The viscosity in PVA and ice is also essentially infinite, but the transitions to C and D still occur. We believe that trehalose plays no special role in the Mb experiments, but that the dehydration prevents the internal motion, and hence also the CO transitions to C and D.

6. Does myoglobin research have a future?

The work of the past few decades that involved myoglobin could lead to the assumption that this field is finished, but we believe that there are a number of directions in which further experiments and computations will yield rich dividends. Even extension of the present work could continue for a considerable time, for instance involving mutants, other heme proteins, other ligands and with different external parameters. We believe, however, that three areas of future research are most promising and important. The first is the effect of protein–protein interactions in protein networks. As pointed out in Section 1, Mb has different functions in the substates A_0 and A_1 [11]. What is the role of the protein network in the control of the function of Mb? The second direction is the search for taxonomic substates in other proteins, such as cytochrome P-450. How are these substates controlled and do they have different structures and functions? The third is a more complete elucidation of the energy landscape, its organization and connection to structure, dynamics and function in a few selected proteins.

Acknowledgments

During the course of writing this paper we have had many discussions. We particularly thank Peter Wolynes, Angel García, William Eaton, Robert Austin and an unknown referee for their suggestions and input. This research was supported by the Department of Energy, under contract W-7405-ENG-36.

References

[1] L.H. Hartwell, J.J. Hopfield, S. Leibler, A.W. Murray, From molecular to modular cell biology, Nature 402 (1999) 47–52.
[2] S. Fields, Proteomics in genomeland, Science 291 (2000) 1221–1224.
[3] N. Wade, Genome's riddle: few genes, much complexity, The New York Times, F1, 13 February 2001.
[4] T. Misteli, Nuclear structure: protein dynamics: implications for nuclear architecture and gene expression, Science 291 (2001) 843–847.
[5] S.J. Hagen, J. Hofrichter, W.A. Eaton, Protein reaction-kinetics in a room-temperature glass, Science 269 (1995) 959–962.
[6] S.J. Hagen, J. Hofrichter, W.A. Eaton, Geminate rebinding and conformational dynamics of myoglobin embedded in a glass at room temperature, J. Phys. Chem. 100 (1996) 12008.
[7] L. Cordone, M. Ferrand, E. Vitrano, G. Zaccai, Harmonic behavior of trehalose-coated carbonmonoxy myoglobin at high temperature, Biophys. J. 76 (1999) 1043–1047.
[8] J.C. Kendrew, R.E. Dickerson, B.E. Strandberg, et al., Structure of myoglobin, Nature 185 (1960) 422–427.
[9] E. Antonini, M. Brunori, Hemoglobin and Myoglobin in their Reactions with Ligands, North Holland, Amsterdam, 1971.
[10] M. Brunori, Structural dynamics of myoglobin, Biophys. Chem. 86 (2000) 221–230.
[11] H. Frauenfelder, B.H. McMahon, R.H. Austin, K. Chu, J.T. Groves, The role of structure, energy landscape, dynamics, and allostery in the enzymatic function of myoglobin, Proc. Natl. Acad. Sci. USA 98 (2001) 2370–2374.
[12] M. Brunori, F. Cutruzzolà, C. Savino, C. Travaglini-Allocatelli, B. Vallone, Q.H. Gibson, Does picosecond protein dynamics have survival value?, Trends Biochem. Sci. 24 (2001) 253–255.
[13] R.H. Austin, K.W. Beeson, L. Eisenstein, H. Frauenfelder, I.C. Gunsalus, Dynamics of ligand-binding to myoglobin, Biochemistry 14 (1975) 5355–5373.
[14] B.P. Schoenborn, H.C. Watson, J.C. Kendrew, Binding of xenon to sperm whale myoglobin, Nature 207 (1965) 28–30.
[15] R.F. Tilton, I.D. Kuntz, G.A. Petsko, Cavities in proteins: structure of a metmyoglobin–xenon complex solved to 1.9 Å, Biochemistry 23 (1984) 2849–2857.
[16] W. Saenger, Structure and dynamics of water surrounding biomolecules, Annu. Rev. Biophys. Chem. 16 (1987) 93–114.
[17] J.A. Rupley, G. Careri, Protein hydration and function, Adv. Protein Chem. 41 (1991) 37–172.
[18] B.P. Schoenborn, A. Garcia, R. Knott, Hydration in protein crystallography, Prog. Biophys. Mol. Biol. 64 (1995) 105–119.
[19] G. Otting, E. Liepinsh, K. Wuethrich, Protein hydration in aqueous solution, Science 254 (1991) 974–980.
[20] V.P. Denisov, B. Halle, Protein hydration dynamics in aqueous solution, Faraday Discuss. 103 (1996) 227–244.
[21] D.I. Svergun, S. Richard, M.H.J. Koch, Z. Sayers, S. Kuprin, G. Zaccai, Protein hydration in solution: experimental observation by X-ray and neutron scattering, Proc. Natl. Acad. Sci. USA 95 (1998) 2267–2272.
[22] J. Fitter, The temperature dependence of internal molecular motions in hydrated and dry alpha-amylase: the role of hydration water in the dynamical transition of proteins, Biophys. J. 76 (1999) 1034–1042.
[23] V.A. Makarov, B.K. Andrews, P.E. Smith, B.M. Pettitt, Residence times of water molecules in the hydration sites of myoglobin, Biophys. J. 79 (2000) 2966–2974.

[24] X. Cheng, B.P. Schoenborn, Neutron-diffraction study of carbonmonoxy myoglobin, J. Mol. Biol. 220 (1991) 381–399.
[25] V. Lounnas, B.M. Pettitt, G.N. Phillips, A global-model of the protein–solvent interface, Biophys. J. 66 (1994) 601–614.
[26] V.P. Denisov, J. Peters, H.D. Hoerlein, B. Halle, Using buried water molecules to explore the energy landscape of proteins, Nat. Struct. Biol. 3 (1996) 505–509.
[27] Y. Shibata, H. Ishikawa, S. Takahashi, I. Morishima, Time-resolved hole-burning study on myoglobin: fluctuation of restricted water within distal pocket, Biophys. J. 80 (2001) 1013–1023.
[28] V. Šrajer, Z. Ren, T.-Y. Teng, et al., Protein conformational relaxational and ligand migration in myoglobin: a nanosecond to millisecond molecular movie from time-resolved Laue X-ray diffraction, Biochemistry 40 (2001) 13802.
[29] B. Gavish, M.M. Werber, Viscosity-dependent structural fluctuations in enzyme catalysis, Biochemistry 18 (1979) 1269–1275.
[30] D. Beece, D.L. Eisenstein, H. Frauenfelder, et al., Solvent viscosity and protein dynamics, Biochemistry 19 (1980) 5147–5157.
[31] A. Ansari, C.M. Jones, E.R. Henry, J. Hofrichter, W.A. Eaton, The role of solvent viscosity in the dynamics of protein conformational changes, Science 256 (1992) 1796–1798.
[32] A. Ansari, C.M. Jones, E.R. Henry, J. Hofrichter, W.A. Eaton, Conformational relaxation and ligand-binding in myoglobin, Biochemistry 33 (1994) 5128–5145.
[33] S. Yedgar, C. Tetreau, B. Gavish, D. Lavalette, Viscosity dependence of O_2 escape from respiratory proteins as a function of cosolvent molecular-weight, Biophys. J. 68 (1995) 665–670.
[34] T. Kleinert, W. Doster, H. Leyser, W. Petry, V. Schwarz, M. Settles, Solvent composition and viscosity effects on the kinetics of CO binding to horse myoglobin, Biochemistry 37 (1998) 717–733.
[35] B.H. McMahon, PhD Thesis, University of Illinois at Urbana–Champaign, 1996.
[36] I. Schlichting, J. Berendzen, G.N. Phillips, R.M. Sweet, Crystal structure of photolyzed carbonmonoxy myoglobin, Nature 371 (1994) 808–812.
[37] H. Hartmann, S. Zinser, P. Komninos, R.T. Schneider, G.U. Nienhaus, F. Parak, X-Ray structure determination of a metastable state of carbonmonoxy myoglobin after photodissociation, Proc. Natl. Acad. Sci. USA 93 (1996) 7013–7016.
[38] T.Y. Teng, V. Srajer, K. Moffat, Photolysis-induced structural changes in single crystals of carbonmonoxy myoglobin at 40 K, Nat. Struct. Biol. 1 (1994) 701–705.
[39] T.Y. Teng, V. Srajer, K. Moffat, Initial trajectory of carbon monoxide after photodissociation from myoglobin at cryogenic temperatures, Biochemistry 36 (1997) 12087–12100.
[40] K. Chu, J. Vojtchovsky, B.H. McMahon, R.M. Sweet, J. Berendzen, I. Schlichting, Structure of a ligand-binding intermediate in wild-type carbonmonoxy myoglobin, Nature 403 (2000) 921–923.
[41] A. Ostermann, R. Waschipky, F.G. Parak, G.U. Nienhaus, Ligand binding and conformational motions in myoglobin, Nature 404 (2000) 205–208.
[42] E.E. Scott, Q.H. Gibson, J.S. Olson, Mapping the pathways for O_2 entry into and exit from myoglobin, J. Biol. Chem. 276 (2001) 5177–5188.
[43] H. Frauenfelder, S.G. Sligar, P.G. Wolynes, The energy landscapes and motions of proteins, Science 254 (1991) 1598–1603.
[44] H. Frauenfelder, B.H. McMahon, Energy landscape and fluctuations in proteins, Ann. Phys. (Leipzig) 9 (2000) 655–667.
[45] A. Ansari, J. Berendzen, S.F. Bowne, et al., Protein states and protein quakes, Proc. Natl. Acad. Sci. USA 82 (1985) 5000–5004.
[46] J.O. Alben, D. Beece, S.F. Bowne, et al., Infrared spectroscopy of photodissociated carboxymyoglobin at low temperatures, Proc. Natl. Acad. Sci. USA 79 (1982) 3744–3748.
[47] A. Ansari, J. Berendzen, D. Braunstein, et al., Rebinding and relaxation in the myoglobin pocket, Biophys. Chem. 26 (1987) 337–355.
[48] F. Yang, G.N. Phillips, Crystal structures of CO-, deoxy- and met-myoglobins at various pH values, J. Mol. Biol. 256 (1996) 762–774.
[49] I.E.T. Iben, D. Braunstein, W. Doster, et al., Glassy behavior of a protein, Phys. Rev. Lett. 62 (1989) 1916–1919.
[50] J.B. Johnson, D.C. Lamb, H. Frauenfelder, et al., Ligand binding to heme proteins. VI. Interconversion of taxonomic substates in carbonmonoxy myoglobin, Biophys. J. 71 (1996) 1563–1573.
[51] J. Berendzen, D. Braunstein, Temperature-derivative spectroscopy: a tool for protein dynamics, Proc. Natl. Acad. Sci. USA 87 (1990) 1–5.
[52] G.U. Nienhaus, J.R. Mourant, K. Chu, H. Frauenfelder, Ligand binding to heme proteins: the effect of light on ligand binding in myoglobin, Biochemistry 33 (1994) 13413–13430.
[53] E.E. Scott, Q.H. Gibson, Ligand migration in sperm whale myoglobin, Biochemistry 36 (1997) 11909–11917.
[54] J.F. Christian, M. Unno, J.T. Sage, P.M. Champion, E. Chien, S.G. Sligar, Spectroscopic effects of polarity and hydration in the distal heme pocket of deoxymyoglobin, Biochemistry 36 (1997) 11198–11204.
[55] L. Cordone, P. Galajda, E. Vitrano, A. Gassmann, A. Ostermann, F. Parak, A reduction of protein specific motions in co-ligated myoglobin embedded in a trehalose glass, Eur. Biophys. J. 27 (1998) 173–176.
[56] D. Vitkup, D. Ringe, G.A. Petsko, M. Karplus, Solvent mobility and the protein 'glass' transition, Nat. Struct. Biol. 7 (2000) 34–38.

[57] D.A. Case, M. Karplus, Dynamics of ligand binding to heme proteins, J. Mol. Biol. 132 (1979) 343–368.
[58] R. Elber, M. Karplus, Multiple conformational states of proteins: a molecular-dynamics analysis of myoglobin, Science 235 (1987) 318–321.
[59] T. Noguti, N. Gō, Structural basis of hierarchical multiple substates of a protein. II. Monte Carlo simulation of native thermal fluctuations and energy minimization, Proteins 5 (1989) 104–112.
[60] H.A. Kramers, Brownian motion in a field of force and the diffusion model of chemical reactions, Physica (Utrecht) 7 (1940) 284–304.
[61] H. Frauenfelder, P.G. Wolynes, Rate theories and puzzles of heme protein kinetics, Science 229 (1985) 337–345.
[62] P. Hänggi, P. Talkner, M. Borkovec, Reaction-rate theory: 50 years after Kramers, Rev. Mod. Phys. 62 (1990) 251–341.
[63] W. Doster, Viscosity scaling and protein dynamics, Biophys. Chem. 17 (1983) 97–103.
[64] M. Settles, F. Post, D. Muller, A. Schulte, W. Doster, Solvent damping of internal processes in myoglobin studied by specific-heat spectroscopy and flash photolysis, Biophys. Chem. 43 (1992) 107–116.
[65] W. Bialek, R.F. Goldstein, Do vibrational spectroscopies uniquely describe protein dynamics? The case for myoglobin, Biophys. J. 48 (1985) 1027–1044.
[66] J. Friedrich, Hole-burning spectroscopy and physics of proteins, Methods Enzymol. 246 (1995) 226–259.
[67] N. Agmon, J.J. Hopfield, CO binding to heme proteins: a model for barrier height distributions and slow conformational changes, J. Chem. Phys. 79 (1983) 2042–2053.
[68] N. Agmon, G.M. Sastry, A temperature-dependent effective potential explains CO is binding to myoglobin, Chem. Phys. 212 (1996) 207–219.
[69] G.M. Sastry, N. Agmon, Trehalose prevents myoglobin collapse and preserves its internal mobility, Biochemistry 36 (1997) 7097–7108.
[70] P.J. Steinbach, A. Ansari, J. Berendzen, et al., Ligand binding to heme proteins: connection between dynamics and function, Biochemistry 30 (1991) 3988–4001.
[71] E.R. Henry, J.H. Sommer, J. Hofrichter, W.A. Eaten, Geminate recombination of carbon monoxide to myoglobin, J. Mol. Biol. 166 (1983) 443–451.